VOL. 25, NO. 1, 2026, 1-4
elektrika.utm.my
ISSN 0128-4428

ELEKTRIKA
Journal of Electrical Engineering

A Single-Stage Constant-Power Double-Sided LCC Inductive Wireless Power Transfer Battery Charger

Jiabo Yan[1, 2], **Mohd Junaidi Bin Abdul Aziz**[1*], and **Nik Rumzi Nik Idris**[1]

[1]Faculty of Electrical Engineering, Universiti Teknologi Malaysia, Skudai, Johor, Malaysia.
[2]Nanning Engineering Technology Research Center for Power Transmission System of New Energy Vehicle, College of Traffic and Transportation, Nanning University, Nanning, Guangxi, China.

[*]Corresponding author: junaidi@utm.my

Abstract: A Constant-Power (CP) double-sided inductor-capacitor-capacitor (DS-LCC) wireless battery charger without any switch-controlled capacitor (SCC) is proposed in this paper. This CP wireless charger incorporates a semi-active rectifier (SAR) in the secondary side, and a control strategy is developed to achieve CP charging. This design eliminates the need for additional SCCs, reducing cost and system complexity. With the DS-LCC compensation topology, this wireless charger has no safety problem when misalignment. The feasibility of the proposed charger is validated through simulation, demonstrating that efficiency is maintained between 93.0% and 94.0%, which surpasses that of the state-of-the-art DS-LCC CP charger.

Keywords: Constant-Power (CP), Double-sided LCC (DS-LCC), Inductive Power Transfer (IPT), Wireless Power Transfer (WPT)

Article History: received 31 January 2025; accepted 19 March 2025; published 30 April 2026
Digital Object Identifier 10.11113/elektrika.v25n1.674

1. INTRODUCTION

The inductive wireless charging technique transfers energy through inductive coupling, enhancing charging automation and improving safety by eliminating the risks of mechanical wear and electrical sparks. This makes it a suitable charging solution for autonomous electric vehicles.

Traditional constant current (CC) charging has been widely adopted in the battery charger field [1],[2]. However, it has a notable drawback. At the onset of the CC charging process, the power transferred is relatively low because the battery voltage is not high, as demonstrated in Figure 1(a). The output power gradually climbs as the battery voltage increases. The CC charging method cannot fully utilize the design capacity of the grid port and charger, limiting the charging rate.

In order to further increase the charging rate, the constant power (CP) charging method was introduced [3]. Figure 1(b) shows that CP charging profile, which operates at maximum output power to ensure complete utilization of the charger or power source's capacity. This approach enables a higher average charging rate than CC charging and reduces charging period. In addition, CP charging mitigates battery aging issues [4], [5].

To achieve CP charging in wireless power transfer, straightforward approaches such as incorporating additional DC-DC converters have been explored [6],[7]. However, the additional DC-DC stage reduces efficiency while increasing cost and system complexity. To overcome this limitation, several single-stage wireless chargers have been proposed. Among them, single-stage CP wireless chargers utilizing the series-series (S-S) compensation network have been developed [8], [9], [10]. However, when these wireless chargers with the S-S compensation network operate in a misaligned state, they are prone to excessive current, a critical issue that mandates the deployment of enhanced safety protection schemes.

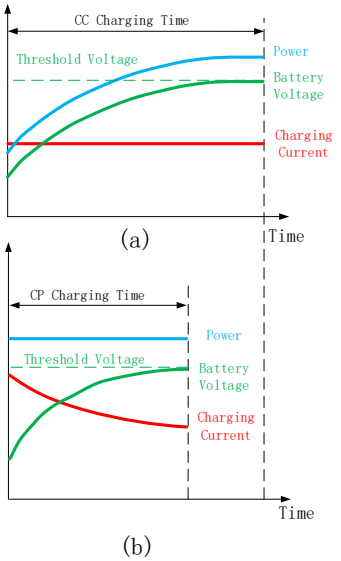

Figure 1. Comparison between (a) CC and (b) CP charging

Wireless charging utilizing the double-sided LCC (DS-LCC) compensation topology effectively addresses this issue while offering several additional advantages, such as a mutual-inductance-independent zero-voltage switching

(ZVS) condition, constant current output character, and high degree of tunability in parameter design [11], [12]. This topology is recommended by industry standards and is widely adopted in industrial field.

However, the traditional single-stage DS-LCC wireless charger can only achieve the CC charging. To fully utilize the power capacity of the charger, the state-of-the-art article [11] introduce two switch-controlled capacitors (SCCs) in the DS-LCC wireless charger to tune the system and achieve CP output. Nevertheless, two additional SCCs in the proposed charger increase both the cost and power loss.

In this study, a new single-stage DS-LCC CP wireless charger is presented, which dispenses with SCCs and consequently achieves a reduction in hardware cost.

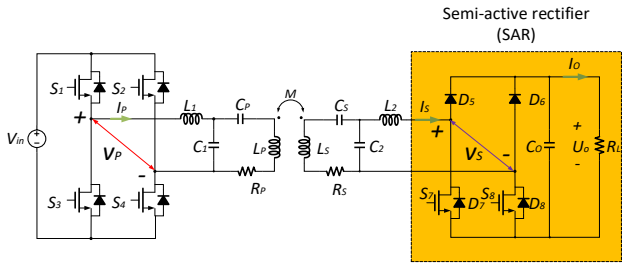

Figure 2. DS-LCC topology structure

2. THE PROPOSED WIRELESS CP CHARGER

2.1 System structure

Figure 2 presents the topology of the proposed IPT wireless charger. On the primary side, four MOSFETs (S_1-S_4), forming an inverter, convert DC to AC. L_1 C_1 C_p, L_p, and R_p serve as the series inductor, parallel capacitor, series-compensated capacitor, self-inductance, and the resistance of the coil, respectively, while L_2 C_2 C_s, L_s, and R_s perform the same functions on the secondary side. A semiactive rectifier (SAR) consists of two diodes D_5 and D_6 and two MOSFETs S_7, S_8 with antiparallel body diodes D_7, D_8. C_o is used as a DC-link capacitor and R_L is represented as an equivalent resistance of the battery. M is the mutual inductance between the two coils and the coupling coefficient k is defined as$k = M/\sqrt{L_p L_s}$. v_p and i_p are the output voltage and current of the inverter; v_s and i_s are the input voltage and current of the rectifier.

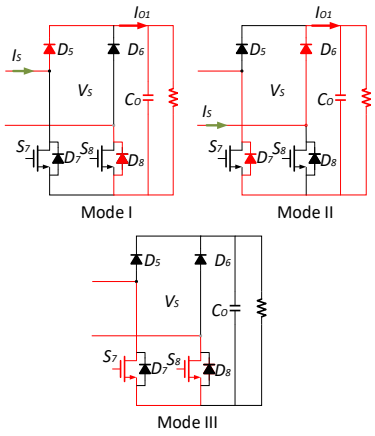

Figure 3. Three modes of the SAR

2.2 Control Method for CP Charging

The SAR operates in three distinct modes: Mode I, Mode II, and Mode III, as illustrated in Figure 3. Mode I and Mode II are just like the traditional diode rectifier, where MOSFETs S_7 and S_8 remain turned OFF. In Mode III, however, S_7 and S_8 are turned ON, forcing v_S to zero during this mode.

The SAR can modulate a square wave v_S with adjustable pulse width W, as shown in Figure 4. Figure 5 shows the corresponding waveforms of i_s and i_{o1}, where pulse width of i_{o1} matches pulse width of v_S. Thus, adjusting pulse width of v_S enables effective control of the output current I_o.

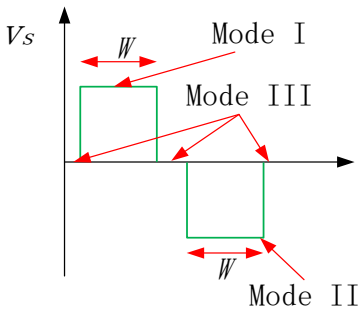

Figure 4. Vs waveform with the SAR operating

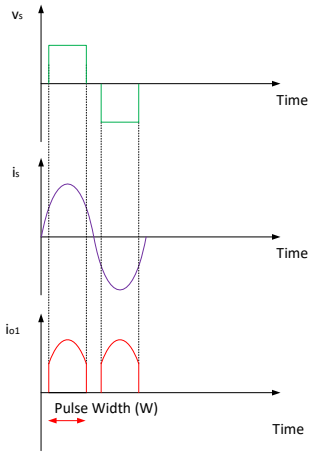

Figure 5. Operating waveforms

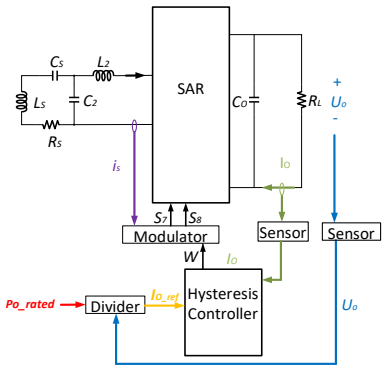

Figure 6. CP control schematic diagram

The proposed CP control schematic diagram is presented in Figure 6. P_{o_rated} represents a predefined rated output power. A divider calculates the reference current

$I_{o,ref}$ based on P_{o_rated} and battery voltage U_o. The reference current I_{o_ref} is employed as the input reference signal. The SAR's input current i_s is utilized by the modulator to detect zero-crossing points and produce the gate drive signals for switch S_7 and S_8.

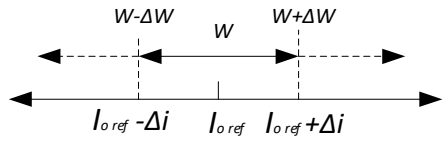

Figure 7. Current regulation control diagram

The hysteresis control algorithm [7] is employed to regulate the current, as illustrated in Figure 7 . If I_o falls below I_{o_ref} - Δi, the controller will increase pulse width (W); if I_o exceeds $I_{o\_ref} + \Delta i$, the controller will decrease W. The current I_o will be kept in the tolerance band. Due to the voltage of battery varies slowly during the charging process

Due to the voltage of battery varies slowly throughout the charging process, the dynamic response of the proposed control method does not represent a key performance requirement. With the proposed control method, the output power is kept at a constant level.

3. SIMULATION

3.1 Specifications

A simulation was carried out in Simulink to validate the effectiveness and feasibility of the proposed CP charger. The passive component parameters were designed following the guidelines in [1].

To simulate the battery voltage U_o within the range of 300–450V, the load resistor, representing the battery, was varied from 15 to 49 Ω based on the battery voltage and rated output power. Detailed experimental specifications are provided in Table 1.

Table 1. Parameters in the simulation

Symbol	Parameter	Value
V_{in}	Input DC voltage	425 V
U_O	Battery voltage (Output DC voltage)	300V-450 V
k	Coupling coefficient	0.32
L_P	Transmitting coil inductance	360 μ H
L_S	Receiving coil inductance	360 μ H
R_{Lp}	Transmitting coil resistance	0.5 Ω
R_{Ls}	Receiving coil resistance	0.5 Ω
L_1	Primary series inductance	67 μ H
L_2	Secondary series inductance	67 μ H
R_{L1}	Primary series inductor resistance	0.1Ω
R_{L2}	Secondary series inductor resistance	0.1 Ω
C_1	Primary parallel capacitance	60.6 nF
C_2	Secondary parallel capacitance	60.6 nF
C_P	Primary series capacitance	14 nF
C_S	Secondary series capacitance	15.1 nF
f	Switching frequency	79 KHz
R_{ON}	MOSFET on-state resistance	0.1 Ω
P_{ref}	Reference power	5KW

3.2 Simulation Results

Figure 8 presents the curves of output power P_o, output current I_o, and output voltage U_o versus the different resistances. During the charging process, the output voltage U_o increases from 300 to 450V, while the output current I_o decreases from 16.67 to 11.11 A. Meanwhile, the output power P_o remains stable within the range of 5063 to 5091 W, demonstrating the achievement of CP output.

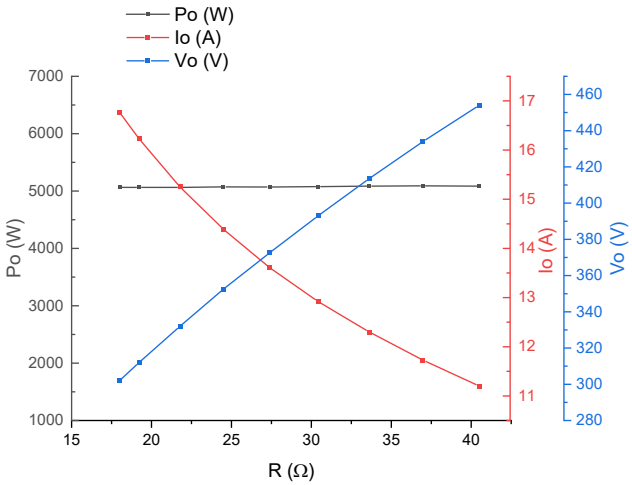

Figure 8. Output voltage V_o, output current I_o, and output power P_o versus the different load reactance in simulation

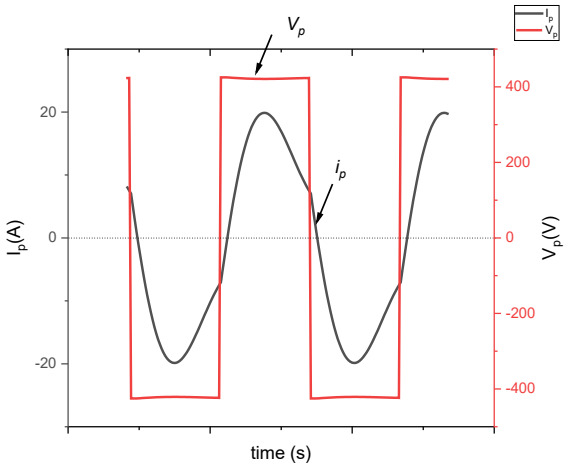

Figure 9. Waveforms of the inverter's input voltage v_p and current i_p

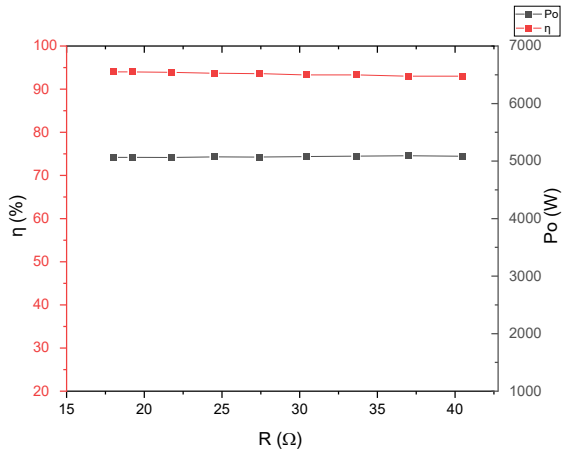

Figure 10. Efficiency and power during the CP Charging

Figure 9 displays the waveforms of the inverter's output voltage v_p and output current I_p, with a phase difference of approximately 10° between them. This indicates that the inverter operates under zero-voltage switching (ZVS), a characteristic inherited from the conventional DS-LCC wireless charger [1].

Throughout the CP charging process, the system maintains an efficiency of 93.0% to 94.0%, as illustrated in Figure 10. This efficiency surpasses the 87.5%–91.5% efficiency reported for the CP wireless charger in [11]. The efficiency comparison among the state-of-the-art CP chargers is demonstrated in Table 2.

Table 2. Features comparison among recent CP chargers

Different Works and Published Year	2020 [9]	2022 [10]	2022 [11]	2024 [5]	This work
Type of Compensation Network	S-S	S-S	DS-LCC	LCC-S	DS-LCC
No Extra Auxiliary SCC	No	Yes	No	Yes	Yes
Efficiency Optimization	Yes	Yes	No	Yes	Yes
No Large Current Issue When Misalignment	No	No	Yes	Yes	Yes
No Wireless Communication	Yes	No	Yes	Yes	Yes
No Noticeable Current Fluctuation	Yes	Yes	Yes	No	Yes
Constant Operating Frequency	Yes	No	Yes	Yes	Yes
Efficiency	88.8%	87.9%	91.5%	89.8%	94.0%

4. CONCLUSION

A CP DS-LCC wireless charger eliminating SCCs is proposed in this paper. The feasibility of the charger is validated by simulation. High efficiency is maintained within the range of 93.0% to 94.0%, which surpasses that of the state-of-the-art DS-LCC CP charger. A comprehensive comparison of recently proposed CP wireless chargers, as shown in Table 2, demonstrates that this constant power wireless charger offers superior overall performance.

ACKNOWLEDGMENT

The authors gratefully acknowledge the financial support in part by the Ministry of Higher Education through Universiti Teknologi Malaysia under the High-Tech Research Grant (Vote No. Q.J130000.4623.00Q21) and the Professional Development Research University Grant (Vote No. Q.J130000.21A2.07E30). This work is also supported in part by the Guangxi Basic Research Capacity Improvement Project for Young and Middle-aged University Teachers (No. 2024KY1879).

REFERENCES

[1] S. Li, W. Li, J. Deng, T. D. Nguyen, and C. C. Mi, "A Double-Sided LCC Compensation Network and Its Tuning Method for Wireless Power Transfer," *IEEE Trans. Veh. Technol.*, vol. 64, no. 6, pp. 2261–2273, Jun. 2015.

[2] V.-B. Vu, D.-H. Tran, and W. Choi, "Implementation of the Constant Current and Constant Voltage Charge of Inductive Power Transfer Systems With the Double-Sided LCC Compensation Topology for Electric Vehicle Battery Charge Applications," *IEEE Trans. Power Electron.*, vol. 33, no. 9, pp. 7398–7410, Sep. 2018.

[3] R. Tanikawa, and H. Le, "Constant power battery charger," *WO1996037941A1*, Nov. 1996.

[4] Z. Huang, S.-C. Wong, and C. K. Tse, "Design of a Single-Stage Inductive-Power-Transfer Converter for Efficient EV Battery Charging," *IEEE Trans. Veh. Technol.*, vol. 66, no. 7, pp. 5808–5821, Jul. 2017.

[5] I.-W. Iam, C.-K. Choi, C.-S. Lam, P.-I. Mak, and R. P. Martins, "A Constant-Power and Optimal-Transfer-Efficiency Wireless Inductive Power Transfer Converter for Battery Charger," *IEEE Trans. Ind. Electron.*, vol. 71, no. 1, pp. 450–461, Jan. 2024.

[6] X. Dai, X. Li, Y. Li, and A. P. Hu, "Maximum Efficiency Tracking for Wireless Power Transfer Systems With Dynamic Coupling Coefficient Estimation," *IEEE Trans. Power Electron.*, vol. 33, no. 6, pp. 5005–5015, Jun. 2018.

[7] Y. Liu, and H. Feng, "Maximum Efficiency Tracking Control Method for WPT System Based on Dynamic Coupling Coefficient Identification and Impedance Matching Network," *IEEE J. Emerg. Sel. Topics Power Electron.*, vol. 8, no. 4, pp. 3633–3643, Dec. 2020.

[8] H. Zhu, B. Zhang, and L. Wu, "Output Power Stabilization for Wireless Power Transfer System Employing Primary-Side-Only Control," *IEEE Access*, vol. 8, pp. 63735–63747, 2020.

[9] Z. Huang, C.-S. Lam, P.-I. Mak, R. P. D. S. Martins, S.-C. Wong, and C. K. Tse, "A Single-Stage Inductive-Power-Transfer Converter for Constant-Power and Maximum-Efficiency Battery Charging," *IEEE Trans. Power Electron.*, vol. 35, no. 9, pp. 8973–8984, Sep. 2020.

[10] F. Xu, S.-C. Wong, and C. K. Tse, "Overall Loss Compensation and Optimization Control in Single-Stage Inductive Power Transfer Converter Delivering Constant Power," *IEEE Trans. Power Electron.*, vol. 37, no. 1, pp. 1146–1158, Jan. 2022.

[11] Z. Luo, Y. Zhao, M. Xiong, X. Wei, and H. Dai, "A Self-Tuning *LCC/LCC* System Based on Switch-Controlled Capacitors for Constant-Power Wireless Electric Vehicle Charging," *IEEE Trans. Ind. Electron.*, vol. 70, no. 1, pp. 709–720, Jan. 2023.

[12] W. Li, H. Zhao, J. Deng, S. Li, and C. C. Mi, "Comparison Study on SS and Double-Sided LCC Compensation Topologies for EV/PHEV Wireless Chargers," *IEEE Trans. Veh. Technol.*, vol. 65, no. 6, pp. 4429–4439, Jun. 2016.